IL NUOVO CIMENTO **40 C** (2017) 90
DOI 10.1393/ncc/i2017-17090-9

COMMUNICATIONS: SIF Congress 2016

Generation, dynamics and coherent structures in RF-generated trapped non-neutral plasmas

G. MAERO(1)(2)(*)

(1) *Dipartimento di Fisica, Università degli Studi di Milano - Milano, Italy*
(2) *INFN, Sezione di Milano - Milano, Italy*

received 28 February 2017

Summary. — In magnetized non-neutral plasmas, features like turbulence and self-organization are observed as a consequence of the Kelvin-Helmholtz instability. With respect to the case of a quiescent single-species distribution and axisymmetric, static boundary conditions, the presence of multiple species and/or the application of radio-frequency (RF) electric perturbations (conditions that may be either unwanted or intentionally pursued) can significantly affect the plasma dynamics and equilibrium. This is the case when the plasma is generated via residual-gas ionization by an external forcing: The interplay of phenomena occurring over different time scales leads to a much more complicated evolution, characterized by the formation of coherent structures and non-axisymmetric final states showing unexpected robustness properties against usual instabilities. The paper discusses the formation of electron vortices reaching an off-axis equilibrium under the continuous application of the RF drive and, through both indirect and direct measurement, shows that a significant fraction of positive ions can be simultaneously confined together with the electron plasma.

1. – Introduction

Magnetized non-neutral plasmas can be efficiently confined in electro-magnetostatic traps, also called Penning or Penning-Malmberg traps, depending on whether the trapping electrostatic potential is harmonic or flat-bottomed [1]. In these devices long-time containment and ease of manipulation and detection, especially with respect to quasi-neutral thermonuclear plasmas, allow experimental physicists to investigate in depth features like turbulence and self-organization arising as a consequence of the diocotron

(*) E-mail: giancarlo.maero@unimi.it

(Kelvin-Helmholtz) instability [2-5]. In particular, initially quiescent single-species distributions are typically injected and let to evolve either freely or subjected to perturbations, *e.g.*, electric fields resonating with plasma modes. In such way it is possible to influence the evolution of the sample, exciting instabilities or possibly suppressing them to enhance the trapping efficiency [6-8] and actively control the plasma positioning and density profile [9-11].

The dynamics and equilibrium properties of trapped samples can be drastically altered when the assumption of a single species starting from axisymmetric initial distributions is broken. For instance, this is the case when the plasma is generated via residual-gas ionization by a suitable radio-frequency (RF) forcing [12]: The interplay of phenomena occurring over different time scales, *e.g.*, RF and diocotron oscillation periods, electron heating, electron-neutral collisions, leads to a much more complicated evolution. In particular, the creation of positive ions is expected to drive a bulk instability of the electron plasma column [13,14], yet a balance is observed between the particle losses and the continuous replenishment by RF-induced heating and ionization. With respect to coherent structures found in pure electron plasmas, the equilibrium states reached under the continuous application of such RF drives show new features including unexpected robustness properties against usual instabilities and, in turn, enhanced lifetime [15].

The understanding and control of instabilities, and as a consequence the opportunity to improve the confinement and possibly manipulate the dynamics of different co-trapped species plays a fundamental role in some of the most challenging applications of Penning traps, like low-uncertainty atomic and nuclear measurements [16, 17], antimatter production [18-20], and two-fluid plasma states [21]. These issues are also relevant to other quasi-neutral or partially neutralized systems characterized by $\vec{E} \times \vec{B}$ dynamics, *e.g.*, thrusters [22], negative ion sources [23] or linear plasma devices [24].

In the following sect. **2** the set-up and the basic features of the RF plasma generation are outlined. Section **3** deals with the analysis of a particularly interesting equilibrium state, namely a single off-axis vortex whose oscillation may be frequency- and amplitude-modulated. Since an assessment of the role played by positive ions is necessary to the understanding of the overall plasma equilibrium, sect. **4** is devoted to experimental observations on the presence of ions, either transient or trapped in the confinement volume. Instability measurements are performed to verify the existence and characterize the nature of ion-driven instability growth, followed by a direct detection of trapped ions. Finally, results and perspectives are summarized in sect. **5**.

2. – Radio-frequency plasma generation

The device used in the experiments is a Penning-Malmberg trap made up of 12 electrodes of radius $R_W = 45\,\mathrm{mm}$. All electrodes from C1 to C8 can be independently set to voltages up to $\pm 100\,\mathrm{V}$ so that an axial electrostatic well with a flexible trapping length up to about 1 m can be obtained, while outer electrodes GND and SH are permanently grounded. The stack, sketched in fig. 1, is enclosed in a vacuum chamber with a residual gas pressure in the 10^{-9}–$10^{-8}\,\mathrm{mbar}$ range surrounded by a solenoid providing a highly uniform axial magnetic field of adjustable intensity $B \leq 0.2\,\mathrm{T}$. At such B field intensity, electrons are highly magnetized, *i.e.* their cyclotron rotation radius and period are very small and this motion can be neglected when compared to the axial oscillation and to the even slower $\vec{E} \times \vec{B}$ transverse drift dynamics.

At the two ends of the stack a charge collector plate and a phosphor screen (biased to a positive voltage $V_{ph} = 3{-}15\,\mathrm{kV}$) can be used to measure the charge and axially-integrated

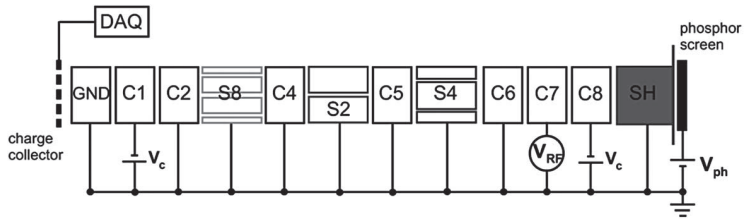

Fig. 1. – Sketch of the trap electrode stack. An example of confining configuration is shown where the electrodes C1 and C8 are set to negative potentials V_c and the RF drive is applied to C7. All other electrodes are grounded. Electrodes S2, S4, S8 are azimuthally split into 2, 4, 8 patches, respectively. A charge collector plate and a phosphor screen (biased to a positive accelerating voltage V_{ph}) are placed at the stack ends.

density profile, respectively, of the plasma flowing out of the confinement volume upon grounding of the respective endcaps. Diocotron modes can be non-destructively monitored via amplification of the current signals induced by the plasma transverse motion on the azimuthally-split electrodes S2, S4 and S8. Further details about the device and typical experimental set-up can be found in previous works [25, 26].

An electron plasma can be generated by setting two electrodes to a confining voltage, generally -80 to -100 V, and one of the intermediate electrodes to a RF sinusoidal drive with 0.5–5 V amplitude and frequency in 1–30 MHz range. In a very simplified view, the axial motion of an electron can be modelled with a one-dimensional iterative map where the particle bounces in a square-bottom potential well perturbed by a square oscillating barrier [12]. Similar map-based models have been studied in the context of classical and quantum oscillators and have been applied to plasma heating in RF discharges [27,28]. Depending on the initial conditions and map parameters, the particle can exhibit both regular and chaotic orbits, with the latter being accessible for the experimental conditions of the experiments presented here (geometry, RF parameters). Free electrons in the residual gas are therefore subjected to stochastic energy jumps. Pressures around the border of the ultra-high vacuum (UHV) range (10^{-9}–10^{-8} mbar), resulting in electron-neutral collision time scales of tens to hundreds of milliseconds, guarantee that electrons will experience tens to hundreds of thousand axial bounces and explore the entire chaotic region of the phase space, *i.e.* receive an average net energy gain beyond the first ionization threshold of light gases, before collisions can dissipate their kinetic energy. The continuous application of the RF drive results therefore in the accumulation of an electron plasma in the confinement volume, which is detected within hundreds of milliseconds and reaches a generation/loss balance within some seconds, after which the total charge and density profile are stable. Axial energy measurements confirm that the energy distribution functions show high-energy tails in the tens of eV [26], making substantial ionization possible. After the RF drive is switched off, the electron plasma thermalizes to temperatures of 1–2 eV. Systematic measurements aimed at the characterization of the plasmas produced via RF excitation against the experimental parameters are discussed in refs. [25, 26].

While some free electrons are always present in the background gas and are often sufficient to start the heating and ionization process, a small additional ionization favouring the initiation of the discharge can be used in the form of UV light or high voltage on any conductor in the vacuum chamber. The latter is actually unavoidable if optical

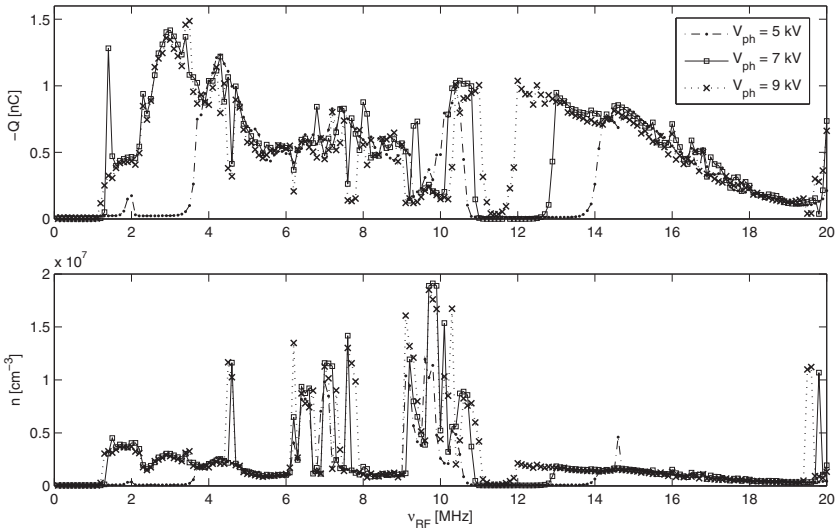

Fig. 2. – Parametric dependence of confined plasma on the phosphor screen voltage V_{ph} as a function of the excitation frequency ν_{RF}. The total charge (top) and mean core density (bottom) of the electron plasma is measured after 4.5 s of confinement and continuous application of a 1.5 V drive on the electrode adjacent to one of the endcaps. Trapping length 570 mm, $B = 0.1$ T.

diagnostics is required, as the phosphor screen must be set to a potential higher than 3 kV. A systematic study concerning the influence of the phosphor voltage on the generation of confined electron plasmas is summarized in fig. 2. The production of plasma is evaluated at different RF excitation frequencies in the 0.1–20 MHz range, applying a 1.5 V drive to the C7 electrode while confinement voltages of −80 V are imposed on electrodes C4 and C8 for a time interval of 4.5 s (typically sufficient to reach a stable configuration). The top diagram shows the total confined charge and the bottom diagram the average density over the area of the image whose intensity is larger than half of the peak value, *i.e.* a rough estimate of the plasma core density, which allows a fast identification of high-density structures with respect to the more frequent diffuse, lower-density plasmas. Curves obtained at $V_{ph} = 5$, 7 and 9 kV show that an increase in the phosphor voltage results in an extended range of frequencies where plasma production is observed. Nevertheless, frequency bands exist where plasma is detected regardless of the value of V_{ph}, and the values of total charge and density are in rather good agreement for all curves, with the exception of RF frequencies yielding high density peaks. This indicates that the ionization due to the phosphor high voltage is helpful in initiating the discharge, which results in easier production of appreciable confined plasma samples, although it is small enough not to influence the successive accumulation of charge, so that the same final equilibrium state is reached if the discharge is started. This consideration will be reprised in the discussion concerning the ion-driven bulk instability in sect. **4**.

3. – Stable and modulated off-axis equilibrium

The formation and accumulation of the electron plasma under the continuous application of the RF drive can be followed by successive dumps on the phosphor screen at increasing confinement times. Diffuse plasmas covering a large part or the entirety of the trap cross section are most frequently observed, sometimes exhibiting density

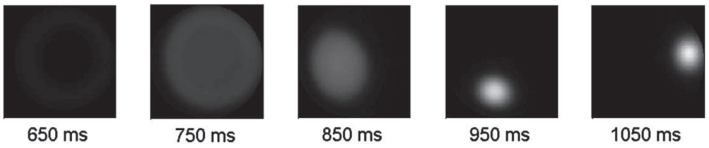

Fig. 3. – Formation of confined electron plasma. Electrons are dumped onto the phosphor screen after increasing time intervals of confinement under the action of an RF drive until a stable configuration is reached. Experimental parameters: 2.5 V quadrupolar RF drive at 12.7 MHz, trapping length 900 mm, $B = 0.1$ T.

inhomogeneities in the form of a denser core within a more diffuse background. The core can exhibit low-order diocotron perturbations (elliptical or triangular shape) later smeared out in the vorticity background. A more interesting phenomenon is the transition to high-density structures occurring for specific sets of parameters (chosen empirically). This is the case of the plasma formation sequence displayed in fig. 3. After the formation of a diffuse plasma starting from the outer regions, where the higher RF field allows for larger heating and ionization, and the accumulation of charge over the whole cross section, the transverse distribution evolves towards an off-axis column with a final radius $R_p \leq 0.2 \cdot R_W$ and peak number density of about $10^7\,\mathrm{cm}^{-3}$. Due to the displacement from the axis the vortex displays a bulk $\vec{E} \times \vec{B}$ rotation, *i.e.* the so-called $l = 1$ diocotron mode [29] with a frequency

$$\nu_1 = \frac{\lambda_p}{4\pi^2 \epsilon_0 B R_W^2} \frac{1}{1 - (D/R_W)^2} \tag{1}$$

which depends on the linear charge density $\lambda_p = Q_p/L_p$ (Q_p and L_p being the plasma charge and density), the magnetic field B, and the radial displacement D.

In freely-evolving off-axis columns, the first diocotron mode can be destabilized, *e.g.*, by the presence of oppositely-charged particles or resistive-wall dissipation. The instability manifests as a growth of the mode amplitude, *i.e.* of the radial displacement, ultimately leading to the loss of plasma on the trap electrodes' wall. On the contrary, the striking feature observed in RF-generation experiments is that as long as the RF drive is applied, the $l = 1$ mode is stable, *i.e.* the rotation continues indefinitely at constant displacement, and hence frequency. Occasionally, an amplitude and frequency modulation of the $l = 1$ signal is detected, with typical modulation frequencies in the $1 - 10$ Hz range. By the combination of electrostatic and optical diagnostics, this modulation can be associated to a periodic variation of both radial displacement and charge of the electron column. The oscillations of the two quantities along the modulation period appear to be phase-shifted with respect to each other. More details about the observation of this phenomenon are reported in ref. [15].

Due to the complexity of the system and the wide range of time scales involved in the process, a unified description of the RF generation from the plasma formation to the attainment of the equilibrium state is not available yet. Nonetheless a very basic model which justifies the existence of a stable, or possibly modulated, equilibrium can be drawn starting from the equation for the fluid (guiding-center) drift motion of the column, $\vec{v} = \vec{E} \times \vec{B}/B^2$, where $\vec{v}$ is the rotation velocity of the column, and the electric field $\vec{E}$ acting on the column is the one from the image charge of the column contained within the circular boundary (trap electrode), approximated as an infinitely thin rod of

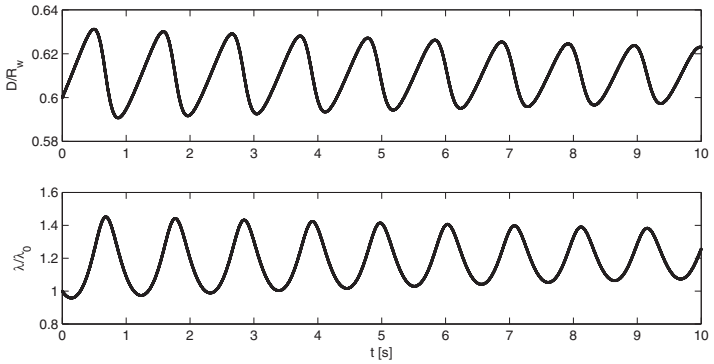

Fig. 4. – Oscillations of the electron column displacement D and linear charge density λ in a guiding-center model. Parameters: $B = 0.05\,\mathrm{T}$, initial charge $\lambda_0 = 1\,\mathrm{nC/m}$, production coefficient $\alpha = 1.1 \cdot 10^3\,\mathrm{m^{-1}s^{-1}}$.

charge. In order to account for the diocotron instability a dissipation must be introduced; to further simplify the problem, a viscous-like force can be used in the form $\mathrm{d}\vec{v}/\mathrm{d}t = -\beta\vec{v}$ (in a later stage, mechanism-specific, *e.g.* resistive or ion-induced, forms of dissipation could be exploited). With these two equations, the mode amplitude $D(t)$ would grow until the plasma hits the wall. The critical ingredient is the hypothesis that the total charge of the column can vary, and that the net variation of the charge depends on the radial position of the column, *i.e.* $\mathrm{d}\lambda_p/\mathrm{d}t = f(D)\lambda$. This assumption is justified on the basis of experimental observations. The vortex charge is the consequence of a balance between continuous ionization and losses of particles. Axial electron losses are detected as a continuous current of electron whose energy overcomes the endcap barrier. Radial losses can also be present, but have not been measured yet. Both loss mechanisms depend on the radial coordinate, but this dependence may be difficult to establish, both experimentally and theoretically. Let us assume that a radial position $D_0 \in [0, R_W]$ exists where the balance between losses and replenishment is zero and linearize $f(D)$ around this position, *i.e.* $f(D) = \alpha(D - D_0)$. Numerical integration of this set of equations shows that depending on the initial conditions, *i.e.* the plasma displacement and charge, both stable and underdamped oscillating solutions can be found around an equilibrium configuration $(\lambda_{p,eq}, D_{eq})$. Figure 4 displays an example using realistic plasma parameters, with a dissipation coefficient consistent with typical instability rates $\simeq 1\,\mathrm{s^{-1}}$, and estimating the magnitude of the production coefficient α from the measurement of the axial electron current. Displacement and charge show a weakly-damped, phase-shifted oscillation with a period just below 1 Hz.

4. – Ion confinement and ion-driven diocotron instability

While for a single-species plasma the conservation of the canonical angular momentum implies the conservation of the mean square radius of the plasma, thus ensuring radial confinement, in the presence of a second sample the mean square radius is conserved only globally. Therefore exchanges in angular momentum are possible between two species, and growth of the mean radius of a positive ion fraction in the electron plasma will destabilize the $l = 1$ electron bulk rotation.

Ions can drive the $l = 1$ instability via substantially different mechanisms, and their relevance to the RF-generated plasma must be assessed. Concerning the transient ion

resonance process [13, 30], due to ions crossing the confinement volume, calculations for the typical parameters of dense vortices [31] predict linear growth rates below $10^{-3}\,\mathrm{s}^{-1}$, which would be masked by diffusion and are hence not detectable.

Another instability mechanism is based on the effect of ions trapped in the confinement region. Although in principle axial confinement is possible only for electrons due to the negative biasing of the endcaps, a nested-trap configuration can be created applying a positive voltage to a pair of electrodes beyond the endcaps, so that ions can be confined. A model was presented in ref. [14] relating the exchange in angular momentum to the different axial oscillation lengths of electrons, confined between endcaps, and ions, whose motion extends within the endcaps. The instability is characterized by an exponential growth rate γ_1 according to the expression

$$\gamma_1 = \frac{N_i}{N_e}\nu_1 \left[1 - \cos\left(2\pi\frac{\tau_{end}}{\tau_{bnc}}\right)\right], \tag{2}$$

where N_i and N_e are the numbers of trapped ions and electrons, respectively, ν_1 the $l = 1$ mode frequency, τ_{bnc} the time spent by an ion to perform an axial oscillation and τ_{end} the portion of such time spent in the endcap regions (forbidden to electrons). Previous experiments reported in ref. [14] were performed in a nested double-trap configuration, inducing some ionization by means of a RF burst exerted on a pre-loaded electron column or by increasing the electron injection energy. Relative ion fractions $N_i/N_e = 10^{-5}$–10^{-4} were estimated from the measurement of the instability growth.

Trapping of ions and the consequent destabilization of the bulk rotation are expected to occur in the case of RF plasma generation, even in the absence of a double-trap configuration. Indeed, a ground potential outside the electron endcaps is sufficient for the negative space charge potential of the electron plasma to create an effective well for positive particles with sufficiently low energy. Typical plasmas with densities of 10^6–$10^7\,\mathrm{cm}^{-3}$ generate negative potentials of some volts, and ions created in the trapping region by ionization with the residual gas will likely retain the average kinetic energies of the gas at room temperature, *i.e.* tens of meV. The application of a RF drive for time spans of seconds suggests the possibility of accumulation of positive ions, leading to more consistent relative ion fractions.

A series of experiments was performed where the plasma was generated in a single-trap configuration, using as endcaps the electrode C8 on one side and varying the length of the endcap on the other side by biasing groups of electrodes, but maintaining the same electron trapping length to alter only τ_{end}. After switching off the RF drive, an exponential growth of the $l = 1$ mode was detected. Growth rates $\gamma_1 = 0.8$–$1.4\,\mathrm{s}^{-1}$, combined with the measured ν_1 and the times τ_{end} and τ_{bnc} estimated for ions experiencing the axial electric field at the radial position of the plasma column, yield relative ion fractions amounting to 10^{-2} and consistent with the functional dependence of eq. 2 within the limits due to shot-to-shot fluctuations of the plasma charge, which give an error of about $\pm 10\%$. The experiments were repeated using $V_{ph} = 6$ and $8\,\mathrm{kV}$ and showed no appreciable dependence on the phosphor voltage, confirming the hypothesis that high-energy transient ions produced by ionization in the phosphor vicinity and repelled by the positive high voltage do not contribute significantly to the instability.

Considering the high ion fraction trapped in the confinement volume, a direct measurement of the ion component was attempted. A diffuse plasma was created in order to maximize the total electron charge and consequently also the absolute number of ions, assuming a similar relative ion fraction could be attained. Once the equilibrium state

was reached, the electron component was dumped onto the phosphor screen by grounding the C8 endcap. After a waiting time of few milliseconds, sufficient to guarantee the complete expulsion of electrons from the trap, the opposite endcap (S8 in this case) was grounded and the adjacent electrode C4 was raised to a positive potential of 100 V to ensure that ions trapped in the endcap region would flow only towards the charge collector. The RC discharge signal measured by an oscilloscope cabled to the collector yielded a positive charge of 8 pC, *i.e.* a fraction $N_i/N_e = 2 \cdot 10^{-2}$ with respect to the electron plasma charge 0.4 nC. This preliminary measurement is qualitatively consistent with the previous indirect measurement method and confirms the possibility to trap a significant amount of positive ions.

5. – Conclusions and outlook

Some peculiar and original features appear when a magnetized non-neutral plasma is generated within the trapping volume of a Penning-Malmberg trap by residual gas ionization. Due to the particular experimental conditions, and specifically the combination of a magneto-electrostatic confinement and the UHV regime, the generation and trapping of an electron plasma are achieved simply exploiting a RF drive of modest amplitude, *i.e.* without the injection of high RF powers common in high-pressure discharges. Due to the presence of the RF drive, a balance between particle production and loss may be established leading to a dynamical equilibrium state with a variety of transverse density distributions. In particular, a stable and dense electron column with an $l = 1$ mode (bulk rotation around the axis) may be observed. The existence of this configuration can be qualitatively justified within a model of $\vec{E} \times \vec{B}$ (guiding center) dynamics as the effect of diocotron mode instabilities inevitably present, *e.g.* due to the presence of positive ions, interacting with a net balance between particle generation and losses influenced by the spatial dependence of the static and RF electric fields. This equilibrium supports the existence of a frequency and amplitude modulation of the $l = 1$ mode, associated with phase-shifted, low-frequency oscillation of the plasma radial displacement and total charge.

The determination of the fraction of trapped ions is also carried out, showing that the positive particle fraction confined in the trap is the dominant instability mechanism for dense electron columns. Through the measurement of instability growth rates, relative ion fractions up to 10^{-2} are estimated. Trapping of such unprecedented ion fractions is directly related to the RF generation mechanism. A scheme for direct measurement of ions via separate ejection of the trapped plasma components is shown to confirm the indirect estimates.

In perspective, further measurements concerning both electron losses as well as ion trapping and loss dynamics are envisaged to give more quantitative indications in view of model refinements. Furthermore, several features observed in RF-generated plasmas suggest significant manipulation opportunities not present in single-species non-neutral plasmas. For instance, a forthcoming paper will show how a resonant excitation of the modulated equilibrium is an effective way to manipulate displacement and charge. Another interesting option is the excitation and control of higher-order diocotron modes occurring during the formation stage of the electron plasma. Finally, while so far the focus has been on the properties of the electron plasma, trapping of large ion samples will be investigated to explore their limitations in terms of total charge and lifetime and the associated possibilities of active control.

* * *

The author acknowledges useful discussions with R. Pozzoli, M. Romé and M. Cavenago, the help and enthusiasm of his students A. Da Col and E. Villa, and the financial support from the INFN Group V projects 'COOLBEAM' and 'PLASMA4BEAM' and from the Piano Sviluppo UNIMI 2014–2016.

REFERENCES

[1] Malmberg J. H. and deGrassie J. S., *Phys. Rev. Lett.*, **35** (1975) 577.
[2] Driscoll C. F., Schecter D. A., Jin D. Z., Dubin D. H. E., Fine K. S. and Cass A. C., *Phys. A*, **263** (1999) 284.
[3] Kawai Y., Kiwamoto Y., Soga Y. and Aoki J., *Phys. Plasmas*, **14** (2007) 102106.
[4] Bettega G., Pozzoli R. and Romé M., *New J. Phys.*, **11** (2009) 053006.
[5] Romé M., Chen S. and Maero G., *Plasma Sources Sci. Technol.*, **25** (2016) 035016.
[6] Hollmann E. M., Anderegg F. and Driscoll C. F., *Phys. Plasmas*, **7** (2000) 2776.
[7] Maero G., Paroli B., Pozzoli R. and Romé M., *Phys. Plasmas*, **18** (2011) 032101.
[8] Kabantsev A. A., Chim C. Y., O'Neil T. M. and Driscoll C. F., *Phys. Rev. Lett.*, **112** (2014) 115003.
[9] Fajans J., Gilson E. and Friedland L., *Phys. Rev. Lett.*, **82** (1999) 4444.
[10] Danielson J. R., Dubin D. H. E., Greaves R. G. and Surko C. M., *Rev. Mod. Phys.*, **87** (2015) 247.
[11] Gomberoff K., Higaki H., Kaga C., Ito K. and Okamoto H., *Phys. Rev. E*, **94** (2016) 043204.
[12] Paroli B., De Luca F., Maero G., Pozzoli R. and Romé M., *Plasma Sources Sci. Technol.*, **19** (2010) 045013.
[13] Fajans J., *Phys. Fluids B*, **5** (1993) 3127.
[14] Kabantsev A. A. and Driscoll C. F., *Fusion Sci. Technol.*, **51** (2007) 96.
[15] Paroli B., Maero G., Pozzoli R. and Romé M., *Phys. Plasmas*, **21** (2014) 122102.
[16] Kluge H. J., Beier T., Blaum K., Dahl L., Eliseev S., Herfurth F., Hofmann B., Kester O., Koszudowski S., Kozhuharov C., Maero G., Nörtershäuser W., Pfister J., Quint W., Ratzinger U., Schempp A., Schuch R., Stölhker T., Thompson R. C., Vogel M., Vorobjev G., Winters D. F. A. and Werth G., *Adv. Quantum Chem.*, **53** (2008) 83.
[17] Maero G., Herfurth F., Kluge H.-J., Schwarz S. and Zwicknagel G., *Appl. Phys. B*, **107** (2012) 1087.
[18] Gabrielse G., Kalra R., Kolthammer W. S., McConnell R., Richerme P., Grzonka D., Oelert W., Sefzick T., Zielinski M., Fitzakerley D. W., George M. C., Hessels E. A., Storry C. H., Weel M., Mullers A. and Walz J., *Phys. Rev. Lett.*, **108** (2012) 113002.
[19] Gutierrez A., Ashkezari M. D., Baquero-Ruiz M., Bertsche W., Burrows C., Butler E., Capra A., Cesar C. L., Charlton M., Dunlop R., Eriksson S., Evetts N., Fajans J., Friesen T., Fujiwara M. C., Gill D. R., Hangst J. S., Hardy W. N., Hayden M. E., Isaac C. A., Jonsell S., Kurchaninov L., Little A., Madsen N., McKenna J. T. K., Menary S., Napoli S. C., Nolan P., Olchanski K., Olin A., Pusa P., Rasmussen C. O., Robicheaux F., Sacramento R. L., Sarid E., Silveira D. M., So C., Stracka S., Tarlton J., Tharp T. D., Thompson R. I., Tooley P., Turner M., van der Werf D. P., Wurtele J. S. and Zhmoginov A. I., *Hyperfine Interact.*, **235** (2015) 21.
[20] Leefer N., Krimmel K., Bertsche W., Budker D., Fajans J., Folman R., Häffner H. and Schmidt-Kaler F., *Hyperfine Interact.*, **238** (2017) 12.
[21] Kawai S., Himura H., Masamune S. and Aoki J., *Phys. Plasmas*, **23** (2016) 022113.

[22] Smolyakov A. I., Chapurin O., Frias W., Koshkarov O., Romadanov I., Tang T., Umansky M., Raitses Y., kaganovich I. D. and Lakhin V. P., *Plasma Phys. Control. Fusion*, **59** (2017) 014041.
[23] Boeuf J. P., Claustre J., Chaudhury B. and Fubiani G., *Phys. Plasmas* , **19** (2012) 113510.
[24] Iraji D., Ricci D., Granucci G., Garavaglia S., Furno I., Cremona A. and Minelli D., *Fusion Sci. Technol.*, **62** (2012) 428.
[25] Maero G., Chen S., Pozzoli R. and Romé M., *J. Plasma Phys.*, **81** (2015) 495810503.
[26] Maero G., Pozzoli R., Romé M., Chen S. and Ikram M., *JINST*, **11** (2016) C09007.
[27] Mateos J. L., *Phys. Lett. A*, **256** (1999) 113.
[28] Lieberman M. A. and Godyak V. A., *IEEE Trans. Plasma Sci.*, **26** (1998) 955.
[29] Davidson R. C., *An Introduction to the Physics of Nonneutral Plasmas* (Addison-Wesley Publishing Company) 1990.
[30] Peurrung A. J., Notte J. and Fajans J., *Phys. Rev. Lett.*, **70** (1993) 295.
[31] Gavassino L., *Sul trasporto di momento angolare all'interno della trappola di Penning-Malmberg* Master's Thesis Università degli Studi di Milano Italy (2016).